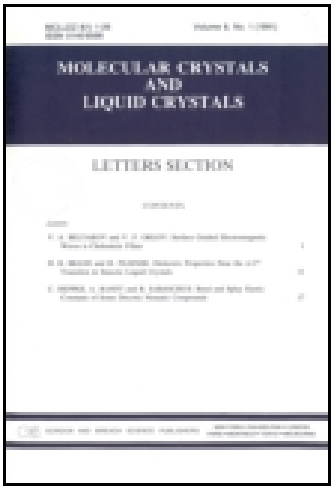


Molecular Crystals and Liquid Crystals
Publication details, including instructions for authors and subscription information:
http://www.tandfonline.com/loi/gmcl20

# Active and Passive LC Based Polarization Elements

J. Stumpe[ab], O. Sakhno[a], Y. Gritsai[a], R. Rosenhauer[a], Th. Fischer[a], M. Rutloh[b], F. Schaal[c], S. Weidenfeld[c], M. Jetter[c], P. Michler[c], C. Pruss[c] & W. Osten[c]

[a] Fraunhofer Institute for Applied Polymer Research, Potsdam, Germany

[b] University of Potsdam, Inst. of Chemistry, Potsdam, Germany

[c] Universität Stuttgart, ITO and IHFG, Stuttgart, Germany

Published online: 30 Sep 2014.

To cite this article: J. Stumpe, O. Sakhno, Y. Gritsai, R. Rosenhauer, Th. Fischer, M. Rutloh, F. Schaal, S. Weidenfeld, M. Jetter, P. Michler, C. Pruss & W. Osten (2014) Active and Passive LC Based Polarization Elements, Molecular Crystals and Liquid Crystals, 594:1, 140-149, DOI: 10.1080/15421406.2014.917503

To link to this article: http://dx.doi.org/10.1080/15421406.2014.917503

*Mol. Cryst. Liq. Cryst.*, Vol. 594: pp. 140–149, 2014

ISSN: 1542-1406 print/1563-5287 online
DOI: 10.1080/15421406.2014.917503

Taylor & Francis
Taylor & Francis Group

# Active and Passive LC Based Polarization Elements

J. STUMPE,[1,2,*] O. SAKHNO,[1] Y. GRITSAI,[1]
R. ROSENHAUER,[1] TH. FISCHER,[1] M. RUTLOH,[2] F. SCHAAL,[3]
S. WEIDENFELD,[3] M. JETTER,[3] P. MICHLER,[3] C. PRUSS,[3]
AND W. OSTEN[3,*]

[1]Fraunhofer Institute for Applied Polymer Research, Potsdam, Germany
[2]University of Potsdam, Inst. of Chemistry, Potsdam, Germany
[3]Universität Stuttgart, ITO and IHFG, Stuttgart, Germany

*Passive and active polarization elements were created by surface and bulk photo-alignment of LCs, reactive LCs, photo-sensitive LCP and photo-curable monomer/LC composites. The use of different photo-sensitive liquid crystalline materials for the development of highly anisotropic elements with high spatial resolution and stability or, alternatively, fast switch ability will be discussed. Photo-active and voltage tunable polarization and diffraction elements are presented. For active micro-optic application a photo-addressed patterned retarder was created. Electrically switchable diffraction gratings were generated by interference exposure of photo-curable LC composites at room temperature characterized by droplet free morphology. These polarization sensitive diffraction elements are characterized be excellent optical properties and low switching times.*

**Keywords** Polarization elements; diffractive elements; polarization gratings; switchable retarder; polymer/LC composites; electrically switchable gratings.



## 1. Introduction

In nature, minerals and biological systems are well-known for their direction dependent properties. Up to now anisotropy of materials and functional systems is not used to a high extent in present technologies, but this is still a large potential for future technological progress. This is of special importance for optical technologies. Organic anisotropic layers or functional elements offer a lot of advantages compared to inorganic ones. First of all organic anisotropic elements are cheaper and easier to process allowing solvent based processing such as spin coating, doctor blading or slot die coating. Their anisotropic properties, i.e. retardation, dichroism or anisotropic emission are often based on the liquid crystalline state. Such materials allow a lower thickness as foil sheets and they offer the possibility to create stacks of functional layers realizing complex structured architectures. Moreover, the materials can be optically processed and in this way anisotropy can locally be varied. Such property can not be achieved for foil polarization sheets.

*Address correspondence to joachim.stumpe@iap.fraunhofer.de; osten@ito.uni-stuttgart.de

On the other hand, new optical technologies require such advanced materials and advanced processing methods to create smaller, thinner, more efficient, multifunctional or smart elements. This is also a large potential for further miniaturization, integration and multi-functionality. Recent progress in optics is significantly driven by polarization and diffraction optics. Another mega trend refers to active, e.g. tunable and switchable or stimuli responsive optics. Smart optical thin film elements based on multifunctional materials and proper patterning are able to overcome restrictions of conventional optics and large mechanical devices. So, the development of tunable and switchable optics is an important trend of technological progress. Ability for tuning is a domain of soft matter and especially of organic materials. Under this aspect LCs with their extraordinary combination of order and mobility are of special importance. A wide range of applications in optics and photonics will exceed the display application. For this purpose we have developed active polarization and diffraction elements varied by light or voltage. In this way retardation or diffraction can be reversibly switched or tuned.



## 2. Permanent Polarisation Elements Based on RMMs and Photosensitive LC Polymers

Two types of LC materials were developed for the fabrication of passive polarization elements: cross-linkable liquid crystalline monomers, so-called reactive mesogen mixtures (RMMs) and liquid crystalline polymers (LCPs) [1–7]. Mixtures of reactive mesogens were typically aligned by interaction with anisotropic surfaces e.g. rubbed polyimides or linearly polarized irradiated photo-alignment layers. Subsequently, the aligned RMM layers are fixed by photo-crosslinking. In the latter case the process is specified as surface photo-alignment.

Alternatively, the alignment of liquid crystalline polymers is carried out by the interaction of incorporated photosensitive side groups with linearly polarized light. In this way a low degree of anisotropy is generated at room temperature in the glassy state of the polymer. Subsequently to the light-induced structuring, the layers are annealed within the LC phase amplifying the photo-induced order. This process is specified as bulk photo-alignment. Such photosensitive LCP offer the advantages of the glassy state, initially isotropic films can be prepared having a hard, non-sticking surface and they need no additional aligning layer. A variety of different photosensitive LC polymers with different photosensitive groups were developed allowing the induction of reversible and permanent anisotropy. Using such LC materials we developed different polarization elements, such as dichroic layers and polarizers, retardation layers, anisotropic emitting layers and polarization gratings.

## 3. Polarization Gratings

Polarization gratings [4–7] were created upon interference exposure with polarized light using both approaches: surface alignment of RMM (two-layer technology) [4, 5] and bulk alignment of photosensitive LCP (one-layer technology) [6, 7]. In the first case a RMM layer was aligned on a patterned photo-alignment layer. The locally varied anisotropy of the alignment layer was generated by holographic UV exposure. The RMM layer was fabricated by spin-coating from a RMM solution onto the prior structured photo-aligning layer. Micrometer-size periods of modulated alignment direction are suitable to create a periodical variation of the RMM orientation resulting in diffractive properties of the film.

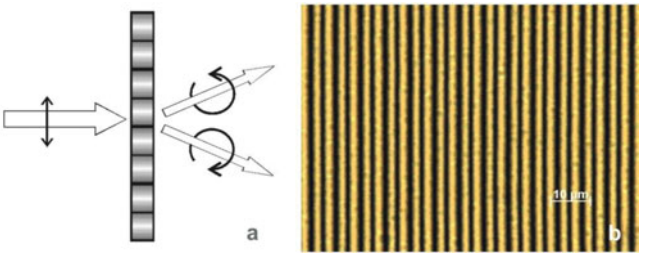


**Figure 1.** Functionality of a polarization grating: a) conversion of linearly polarized beam into left and right handed circular polarized beam and b) polarization grating with a period of 3 $\mu$m between crossed polarizers (1000x) (Picture credits: Fraunhofer IAP).



Subsequently, the layer was fixed by photo-crosslinking. Period and thickness of the RMM layer determine diffraction angle and efficiency.

Polarization gratings made by this method convert a beam of linear polarized light into two beams of circular polarized light with opposite handedness (Fig. 1a). A polarization microscope image of such a polarization grating is shown in Fig. 1b. Quite similar polarization gratings were also generated by the one layer technology due to holographic exposure of a photosensitive LCP. Such polarization gratings can be used as diffractive optical elements in advanced projection systems, light processing devices or analytical instruments.

## 4. Photo-Addressed Retarder for Active Micro-Optics

An active micro-optical system was developed that provides spatial polarization control. In this case polarized light causes an all-optical reorientation of the liquid crystals overcoming restrictions of voltage control requiring pixelated electrodes. As miniaturized light source a set of VCSEL were used. With respect to the VCSEL emission an aligning material which is photoactive in the range of 650 nm is required. For this purpose a push-pull (bis)-azobenzene based photo-addressable aligning materials was developed that introduces local and reversible variation of birefringence in a liquid crystal cell. This leads to an all-optical reorientation of liquid crystals (Fig. 2). The wavelength of the addressing light can be range from near UV up to near IR. Depending on the requirements, the photoactive layer unit can be implemented as a self-assembled multilayer (SAM) or a simple spin-coated polymer film (Fig.3).

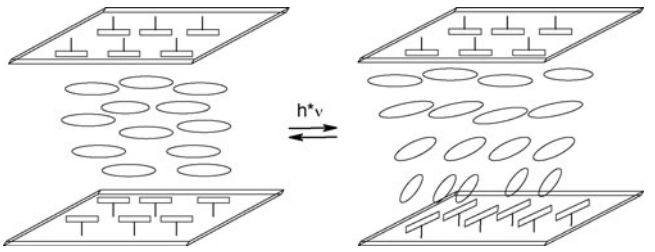


**Figure 2.** Switching process of LC-cell forced by (re)orientation from an azobenzene based aligning layer (downside) due to polarized exposure.

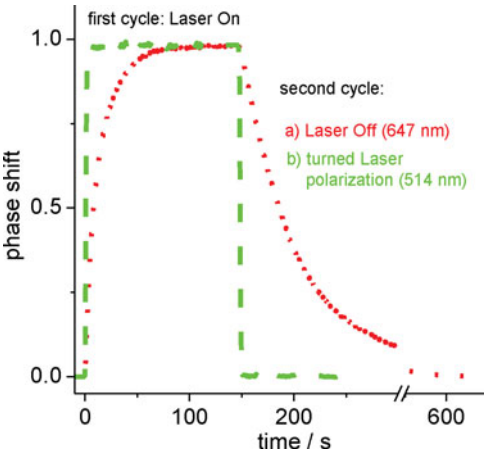


**Figure 3.** Change of retardation of a standard LC mixture during writing and relaxation cycle forced by a photo-addressable aligning layer. a) spin-coated layer addressed @ 647 nm and b) self-assembled layer addressed @ 514 nm

The system (Fig. 4) consists of a photo-addressable layer in conjunction with a commercially available LC mixture (E5) enclosed into a transparent cell, a number of thin film optical elements for light steering and an array of vertical cavity surface emitting lasers (VCSEL) that generates linearly polarized addressing light beams [8, 9]. The addressing patterns are generated by diffractive optical beam shapers. Each beam crosses a DOE forming a polarization pattern in the plane of the photo-addressable layer. Due to the small size of the components it is possible to realize several addressing channels in one device. The addressing beams can be used separately or combined individually which allows switching between different polarization states over a defined area (Fig. 4).

Thus, a probing light beam can be easily tuned in its polarization state. The combination of the micro-optical illumination setup and the newly developed reversible photo-addressable aligning layer enables the fabrication of a micro-optical system which is not limited by pixelation. It offers a highly efficient lateral spatial resolution of $\geq$200 LP/mm (Fig. 5). The complete system can be integrated into a microscope objective allowing a switchable phase contrast (locally variable and reversibly switchable Zernike-Plate).

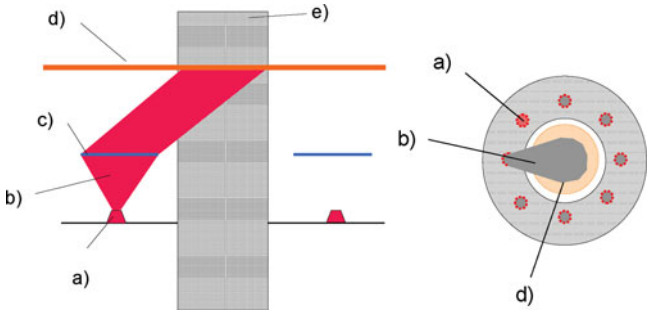


**Figure 4.** Side and II) top view of an active polarization device consisting of an array of a) VCSELs with individually related b) beam forming c) DOEs and a d) photo-addressable unit [6].

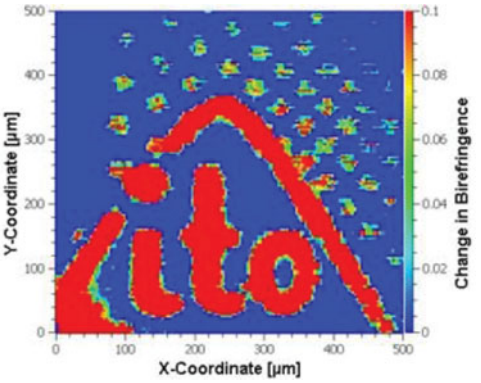


**Figure 5.** Two-dimensional change of birefringence within a photo-addressable unit



## 5. Electrically Switchable Polarization and Diffraction Elements

In addition to passive anisotropic layers and polarization gratings also active, electrically tuneable or switchable elements with polarization dependent performances were developed. For the last case different variants of holographically photo-curable polymer-LC materials were developed. Holographic polymer dispersed liquid crystals (H-PDLC) have been the subject for the creation of electrically switchable/tuneable diffractive elements for optical and photonic applications. Holographic exposure of composites of photoreactive monomers and LCs to an interference pattern leads to diffraction gratings consisting in a sequence of submicron polymer lamellae alternated by areas with PDLC droplets [10–12]. Although the diffraction efficiency of H-PDLCs can be quite high, the gratings reveal either high scattering loss when the droplet size is comparable to the wavelength of light, or rather high values of switching voltage in the case of nanosize droplets. These drawbacks restrict wide practical applications of H-PDLCs.

A new type of switchable holographic gratings with non-droplet morphology consisting of isotropic polymer walls alternated by channels of planar aligned LCs, published under the terms POLIPHEM and POLYCRYPS was proposed some years ago. The two phase, droplet-free morphology of the gratings results in diffraction elements of high diffraction efficiency, negligible light-scattering and excellent electro-optical performance. The preparation of the POLICRYPS gratings requires temperatures above the clearing point of the LC component for phase separation during the holographic exposure [13, 14]. In contrast, POLIPHEM gratings are obtained by one-step all-optical fabrication at room temperature based on proper designed materials and related processing conditions [14, 15].

The POLIPHEM gratings are formed using a homogeneous mixture of photo-curable pre-polymers, nematic LC (Fig. 6) and a photoinitiator. Exposure to an interference pattern causes the formation of a periodic structure of photo-crosslinked polymer network and planar aligned LC. So, pattern-wise photo-polymerization and subsequent phase separation result in the formation of a volume grating. Firstly, the polymer network is formed in the bright regions of the interference pattern. This misbalance causes diffusion of reactive monomers from the dark to the bright fringes replacing the consumed monomers. Simultaneously the LCs undergo a counter-wise diffusion to the dark regions forming planar aligned LC layers, i.e. the LC molecules are planar aligned always perpendicularly to the grating planes, without formation of LC droplets (Fig. 6). While in the initial state the LCs were homogenously mixed with the monomers to an isotropic syrup there is no

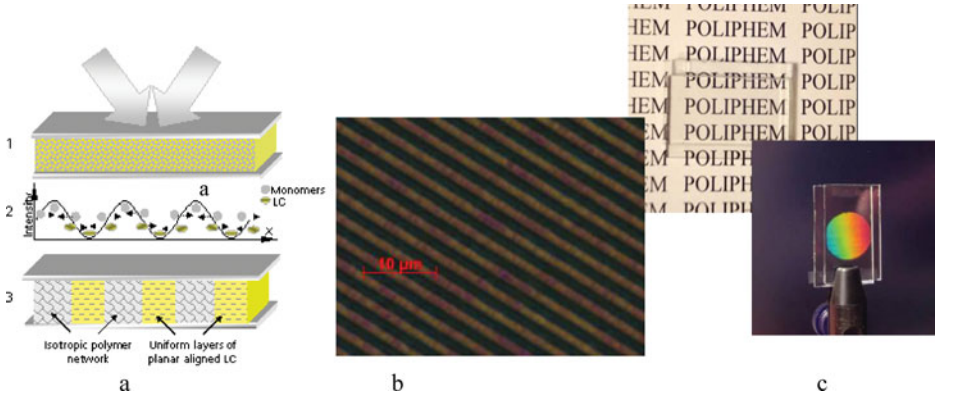


**Figure 6.** (a) Schematic illustration of the formation of POLIPHEMs: 1. initial layer; 2. exposure to an interference pattern: local polymerization of monomers, counter diffusion of monomers and LC, alignment of the LC; 3. resulting structure; b) POL image of a POLIPHEM grating between crossed polarizers, period is 2.3 $\mu$m, c) high optical quality of POLIPHEM gratings.



compatibility of the LC with the photo-generated polymer. Thus the initially homogeneous two-component system is transformed to a non-scattering two-phase system of alternating layers of isotropic polymeric network and uniformly aligned LC (Fig. 6 a). Due to the spatial distribution of the two phases having a large difference in their refractive indices the final gratings possess large refractive index modulation, a high anisotropy (Fig. 6 b) due to the planar orientation of the LC along with excellent optical quality (Fig. 6 c).

The previous POLIPHEM material was based on commercial Norland adhesive NOA68 and 35wt.% of K15 that enables holographic structuring only with UV exposure ($\lambda_{rec}$ = 364 nm) [14, 15]. Recently, a series of home-made monomer-LC composites for the fabrication of POLIPHEM gratings were developed which are based on acrylate and thiol pre-polymers and specific LC components. The new LC component is based on a mixture of several nematic LCs instead of a single nematic LC. The LC content was varied in the range of 30–40 wt.%. Different new photo-initiator systems provide sensitivity of the new materials to UV and vis light allowing the grating fabrication with cheaper vis lasers.

In order to fabricate transmission POLIPHEM gratings the samples, prepared by sandwiching the initial reactive mixture between two glass substrates with transparent ITO electrodes separated with glass spacers of proper thickness ($d$), were illuminated with the interference pattern of two $s$-polarized laser beams of almost equal intensity. With respect to the sensitivity of new materials laser with 364, 488 or 532 nm can be used. Generally, a slow curing regime [16] with enough low recording intensity at temperature of 20–23°C is maintaining during holographic exposure. The evolution of the diffraction efficiency of the POLIPHEM gratings can be monitored in real time during holographic recording by using a 633 nm laser beam at the Bragg angle. The POLIPHEM gratings are thick volume gratings [17], therefore the diffraction efficiency of the grating (DE, $\eta$) was estimated as $\eta^{s,p}(t) = I_{-1}(t)/(I_0(t)+I_{-1}(t))$, where $I_0(t)$ and $I_{-1}(t)$ are the intensity of the transmitted beam (0th diffraction order) and the diffracted beam (–1st diffraction order), respectively.

A typical two-stage time-evolution (monitored with $s$- and $p$-polarized beams) that indicates the formation of the characteristic POLIPHEM grating morphology is shown in Fig. 7 a. Firstly, the diffraction efficiencies of $s$- and $p$-polarized light ($\eta^s$ and $\eta^p$) grow up to a proper value. Starting from this time, $\eta^p$ increases up to almost 98% (Fig. 7 a, gray curve).

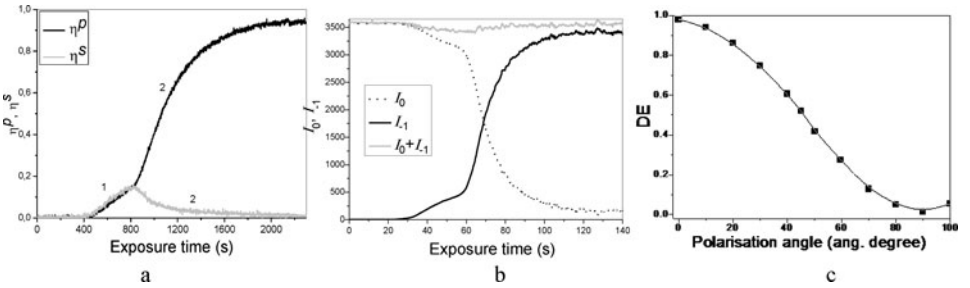


**Figure 7.** a) Typical time-evolution of the diffraction efficiency, monitoring with *s*- and *p*-polarised beams ($\lambda_{rec}$ = 488 nm, period $\Lambda = 1\mu$m, $d = 10$ $\mu$m), b) intensity of transmitted ($I_0$), diffracted ($I_{-1}$) beams and their sum during holographic exposure, monitoring with *p*-polarised beam ($\lambda_{rec}$ = 364 nm, period $\Lambda = 900$ nm, $d = 10$ $\mu$m), c) diffraction efficiency via the orientation of polarisation plane of the incident beam (Grating parameters: period $\Lambda = 1\mu$m, $d = 10$ $\mu$m).



At that $\eta^s$ slowly goes down. The first stage (1) of the curves is attributed to the fast photo-curing of the monomers in the bright regions accomplished with phase separation of the LC from polymer network without the LC alignment. The second stages (2) reflects the progress of a planar alignment of the LCs along the grating vector that provides a drastic growth of $\eta^p$ due to a large mismatch between the extraordinary refractive index of the LC, $n_e$ ($\approx$1.7) and the RI of the polymer, $n_{pol,}$ ($\approx$1.54). In contrast, the final diffraction efficiency of *s*-polarized light is usually less than 1% (Fig. 7 a, grey curve) due to approaching of the polymer index, $n_{pol}$, to the ordinary refractive index of the LC, $n_o$. Thus, the POLIPHEM gratings operate properly with *p*-polarized light only. An *s*-polarised beam does not experience any index modulation across the cell, without and with an electric field. Fig. 7 b indicates a negligible light scattering in the sample during exposure: the sum of the intensities of diffracted and transmitted beams is almost constant (grey line).

The dependence of the diffraction efficiency of a POLIPHEM grating with a 1.0 $\mu$m period on the orientation of the polarisation plane of the incident light is shown in Fig. 7 c. The POLIPHEM gratings with periods in the range of 380–1200 nm and also slant gratings with slant angles up to 40° perform similar polarisation behaviour and show the diffraction efficiency of up to 99% for *p*-polarised light and a negligible diffraction of *s*-polarised light.

The POLIPHEM grating can be switched between a diffractive "On"-state (field-off state) of the highest refractive index contrast and a transmissive, non-diffractive, "Off"-state (field-on state) by applying an external electric field, due to the realignment of the LC molecular director parallel to the field direction. In the initial field-off *p*-polarized light is diffracted with high efficiency due to the largest refractive index difference between the LC and polymer fringes (Fig. 8 a (1)). An applied voltage reorients the aligned LC with positive dielectric anisotropy along the field direction (Fig. 8 a (2)) that decreases the refractive index contrast and diffraction efficiency of *p*-polarised light. At proper voltage ($U_{dr}$) the diffracted beam completely disappears due to an almost complete approaching of $n_{LC}$ to $n_{pol}$. An s-polarised light is not influenced with the field (Fig. 8 a (2)). In contrast to H-PDLCs, the POLIPHEM gratings are transparent in the field-on and -off as well as in all intermediate states. The intensities of the transmitted and the diffracted beams and their sum as a function of an applied voltage is presented in figure7 b: there is a lossless exchange of the input energy between two output beams. The maximum On-/Off-switching contrast, estimated as $\eta^p(0\ V)/\eta^p(U_{dr})$, as high as 200 was achieved.

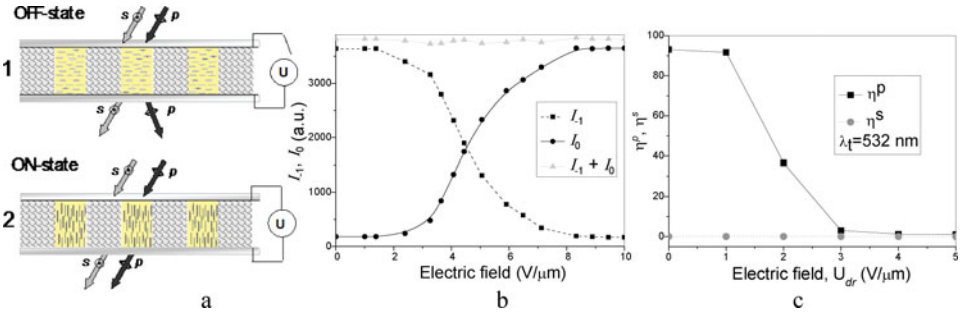


**Figure 8.** a) Electro-optical functionality of POLIPHEM with *p*- and *s*-polarized light; (b) dependence of $I_0$, $I_{-1}$ and $I_0 + I_{-1}$ on an applied voltage obtained with p-polarised beam, the grating in the UV sensitive material (dc, $U_{thr} = 2$ V/$\mu$m, $U_{dr} = 9$ V/$\mu$m); c) voltage dependence of $\eta^p$ and $\eta^s$ of the gratings made in the vis material, monitoring at $\lambda_t = 532$ nm (dc, $U_{thr} = 0.8$ V/$\mu$m, $U_{dr} = 3$ V/$\mu$m).



The basic POLIPHEMs features like high efficiency of *p*-polarised light of a proper wavelength, high grating anisotropy and electric switchability can be used to design an efficient and fast electro-optical chopper for *p*-polarized light or a polarization shutter (Fig. 8). In the field-off state *s*-polarised beam goes through the grating without diffraction in the direction of the 0th diffraction order and *p*-polarised beam diffracts with almost 100% into the 1st order. Applying of a proper driving voltage erases the grating and both beams will be redirected in the direction of the 0th order. Such electro-optical shutters were realized for the operation at different wavelengths in the spectral range from 405 up to 800 nm.

The electro-optical performances of POLIPHEM gratings depend on the material formulation: the comparison was done for the gratings fabricated using the vis and the UV sensitive POLIPHEM materials containing different photoinitiators and fabricated by exposure to 488 and 364 nm wavelengths. Fig. 8 c shows the dependence of $\eta^p$ via the applied voltage of a grating operating at 532 nm. The lowest threshold ($U_{thr}$) and driving voltage ($U_{dr}$) were obtained of about 0.8 and 3 V/$\mu$m, respectively. The corresponding values of $U_{thr}$ and $U_{dr}$ for the samples formed with the UV sensitive material are usually at least of about 2–3-fold higher (fig. 8 b). The shortest Off-On-switching times, $t_{Off}$ and $t_{On}$, of the gratings formed in the UV material of ~80 and ~120 $\mu$s, correspondingly, were obtained. The shortest $t_{Off}$ and $t_{On}$ of ~250 $\mu$s and ~1200 $\mu$s, respectively, were measured for the samples based on the vis sensitive material.

Due to their anisotropic nature POLIPHEM gratings perform the property of phase retarder. It means that light of a wavelength $\lambda$ propagating through the grating, will be separated into an ordinary and an extraordinary components. For a sample of the thickness *d* and the birefringence, $\Delta$n, the phase difference between these two waves will be determined as: $\varphi = 2\pi d\Delta n/\lambda$. The measurements of the birefringence and its electro-optical dependence were performed by placing the grating between crossed polarisers normally to an impinging beam and measuring the intensity of the transmitted beam without and with an applied voltage. The calculations of $\Delta$n were done using the equation: $I_{cross}(U) = I_0 \sin^2(\Delta n \pi d/\lambda)\sin^2 2\alpha$, where $I_{cross}(U)$ is intensity of the transmitted beam, $\alpha$ is the angle between the grating vector and the axes of polarisers and it was equal to 45°, $\lambda = 633$ nm. For the gratings with a period of 1 $\mu$m and thickness of about 10 $\mu$m the value of $\Delta$n was estimated as 0.023. The value of birefringence can be electrically controlled (Fig. 9). A

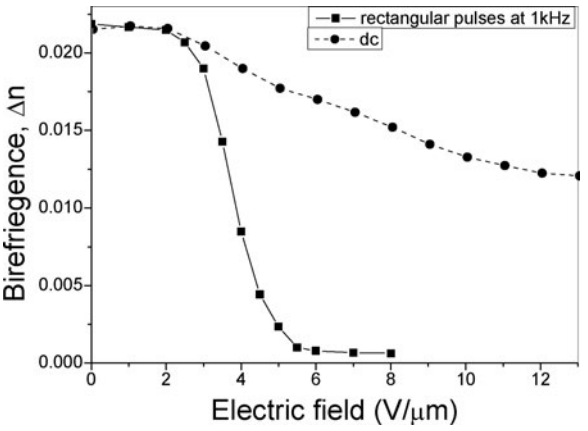


**Figure 9.** Birefringence versus the applied electric field (the measurements with dc voltage and with 1 kHz rectangular pulses). Grating parameters: period $\Lambda = 1\mu$m, $d = 10\ \mu$m.

complete off-switching of the birefringence and lower switching voltage were obtained by applying rectangular voltage pulses at 1 kHz.

## 6. Conclusions

The materials and all-optical photo-processes were developed for the fabrication of liquid crystal based passive and active polarisation elements. Surface and bulk photo-alignment of LCs, reactive LCs and photosensitive LC polymers were used as basic processes. Examples of optical films and diffractive elements are presented. As an example for a passive thin-film element, a permanent polarisation grating is presented which forms due to a photo-alignment of reactive mesogens on a holographically patterned aligning layer or, alternatively, due to interference patterning of photosensitive liquid crystalline polymers with polarized light. As an example for an active polarisation element a photo-addressed retarder was developed using a photo-addressed azobenzene aligning layer by linearly polarized light of a VCSEL array to create spatial polarisation control with a lateral resolution up to 200 LP/mm.

Electrically switchable/tuneable diffractive volume gratings are the second representative of active polarisation elements. The gratings were fabricated using the composites containing photo-curable monomers and nematic LC. Interference exposure at room temperature results in high efficient and tuneable Bragg gratings. The gratings are characterized by excellent optical quality due to their LC-droplets-free morphology. They allow tuning and switching of *p*-polarized light in the sub ms range with low electric fields. The strong dependence of grating parameters on the polarisation of light enables applications as novel electrically-switchable polarisation-dependent diffraction devices. Both passive and active optical elements presented can be used as effective, flexible, low-cost and thin film polymer components in a wide field of application in optics and photonics.

## References

[1] Stumpe, J., Läsker L., Fischer, Th., Kostromin S. & Ruhmann R. (1996). *Thin Solid Films*, *284*, 252.

[2] Rosenhauer, R., Stumpe, J., Gimenez, R., Pinol M., Serrano, J. L. & Vinuales A. (2007). *Macromol. Chem. Rap. Commun.*, *28*, 932.

[3] Rosenhauer, R., Stumpe, J., Giménez, R., Piñol, M., Serrano, J. L., Viñuales, A. & Broer, D. (2011). *Macromolecules*, *44*, 1438.
[4] Escuti, M. J., Oh Ch., S′anchez C., Bastiaansen C. & Broer D. J. (2006). *Proc. of SPIE*, 6302, 630207–1.
[5] Oh, Ch. & Escuti M. J. (2008). *Opt. Lett. 33*, 2287.
[6] Kawatsuki, N.Hasegawa,T., Ono, H. & Tamoto, T. (2003). *Adv. Mat.*, *15*, 991.
[7] Ono, H., Nakamura, M. & Kawatsuki, N. (2007). *Appl. Phys. Lett.*, *90*, 231107.
[8] Eichfelder, M., Schulz, W.-M., Reischle, M., Wiesner, M., Roßbach, R., Jetter, M. & Michler P. (2009). *Appl. Phys. Lett.*, *95*, 131107.
[9] Jetter, M., Roßbach, R. & Michler, P. (2009). *Photon. Internatational*, *1*, 33.
[10] Bunning, T. J., Natarajan L. V., Tondiglia V. P., Sutherland R. L., Veziet D. L. & Adams W. W. (1995). *Polymer Lett.*, *64*, 2699.
[11] Bunning T. J., Natarajan L. V., Tondiglia V. P. & Sutherland R. L. (2000). *Annu. Rev. Mater. Sci.*, *30*, 83.
[12] Liu Y. J. & Sun X. W. (2008). *Advanc. Optoelectron., ID 684349*, 52 pages.
[13] Caputo R., De Sio L., Veltri A., Umeton C. & Sukhov A. V. (2004). *Opt. Lett.*, *29*, 1261.
[14] Abbate G., Vita F., Marino A., Tkachenko V., Slussarenko S. S., Sakhno O.V. & Stumpe J. (2006). *Mol. Cryst. Liq. Cryst.*, *453*, 1.
[15] Sakhno O. V., Slussarenko S. S. & Stumpe, J. (2004). *Proc. SPIE*, *5521* 38.
[16] Veltri A., Caputo R., Umeton C. & Sukhov A. V. (2004). *J. Appl. Phys.*, *84*, 3492.
[17] Gaylord T. K. & Moharam N. G. (1985). *Proc. IEEE*, *73*, 894.